Assiut University Journal of Multidisciplinary Scientific Research (AUNJMSR)
Faculty of Science, Assiut University, Assiut, Egypt.
Printed ISSN 2812-5029
Online ISSN 2812-5037
Vol. 53(1): 119- 135 (2024)
https://aunj.journals.ekb.eg

Application of stripping technique on gravity data to study the structure evaluation in Abu Ghradiq basin and its surroundings, northern Western Desert, Egypt

Mahmoud T. Saad [1], Mahmoud M. Senosy [2] and Haby S. Mohamed [2,*]
Geology Department, Faculty of Science, Assiut University, Assiut, Egypt
[*]Corresponding Author: mahmoud011698@science.aun.edu.eg

ARTICLE INFO

Article History:
Received: 2023-10-01
Accepted: 2023-11-07
Online: 2023-12-28

Keywords:
stripping technique, structure evaluation, Abu Ghradiq basin, northern Western Desert, Application of gravity data.

ABSTRACT

The northern part of the Western Desert, Egypt is an exceptional area since it is a significant hydrocarbon-rich region, containing many potential basins. The study area lies between latitudes 28° 00’ and 30° 30' N, and longitudes 26° 00' and 31° 18' E. The present study employs lithological data from 48 drilled wells and Bouguer gravity data to compute gravity for five distinct sedimentary sequences separated from the well data. The five sequences were classified and designated as Sequences I to V, based on their density contrast. The thickness of each sequence was obtained from the well data. Gravity values for each sequence were calculated using the conventional gravity equation based on thickness and density. By employing the stripping process, gravity associated with each sequence was subtracted from the Bouguer gravity of the area to the basement rocks. A contour gravity anomaly map was generated for each specific sedimentary sequence in addition to the basement rocks. These maps and rose diagrams revealed prevalent structural trends in the east-west (E-W), northeast-southwest (NE-SW), and northwest-southeast (NW-SE) orientations across all sequences. NW-SE trend is the main structural trend in sedimentary sequences, with a slight 5-degree deviation from sequence I to V. In contrast, basement rocks exhibit more complex and varied structural trends. The basement rocks were affected by an early tectonic event, and later both the sedimentary sequences and basement rocks were influenced by another tectonic event. These tectonic phases have created favourable conditions for hydrocarbon generation and accumulation in this area. The intense tectonic activity, which includes processes like subsidence, faulting, and structural traps, has led to the formation of reservoir rocks, source rocks, and migration pathways conducive to hydrocarbon storage. Additionally, the high heat and pressure associated with these tectonic phases have contributed to the transformation of organic material into hydrocarbons over geological time, making the region highly prospective for hydrocarbon exploration.

1. INTRODUCTION

The technique of "deep gravity interpretation by stripping" was discussed by Hammer [1] as a mean of extending gravity interpretations to deeper levels. The stripping method is predicated on a more precise physical basis compared to any other mathematical approach for analysing gravity fields.

The northern part of Western Desert of Egypt is an exceptional area since it is a dominant contributor of hydrocarbons, containing many fascinating and potential basins. Its importance is attributed to the dynamic depositional history which lead to the formation of many depositional basins such as Alam El-Bueib, Matruh, Natrun, Siwa, Abu El Gharadig, and Gindi. Some sedimentary basins have attracted a lot of attention due to their petroleum potential [2].

The main objective of this research is to apply the stripping technique on Bouguer Gravity data of Abu Gharadig basin and its surroundings to study the structure evaluation of this important part of the northern Western Desert. The study area lies between latitudes 28° 00’ and 30° 30' N, longitudes 26° 00' and 31° 18' E (Figure 1.a).

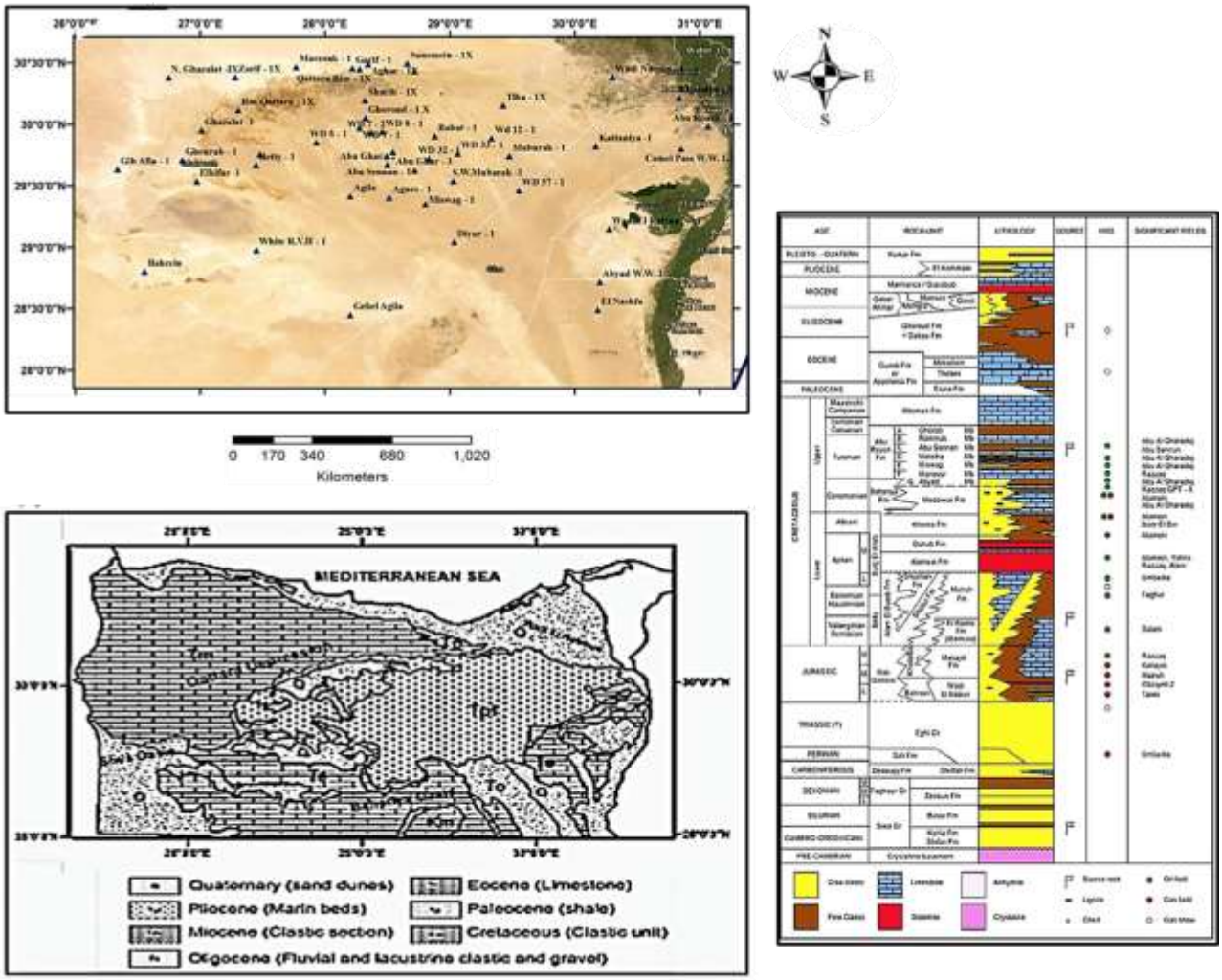

Figure 1a) Location map of the study area, including deep wells; b) Northwestern Desert geological map (adapted from Egypt’s geological map, (25); and c) Northwestern Desert generalized litho-stratigraphic column (Schlumberger (37)).

2. Geologic and structure setting

Many authors have focused on the surface, subsurface structural, and stratigraphical aspects of the Western Desert, among those are, [3], [4], [5], [6], [7], [8], [9], [10], [11], [12], [13], [14], [15], [16], [17], [18] and [19]. All of them have discussed subsurface geology and stratigraphy of the northern Western Desert (see Figure 1c). The thick sedimentary sequence in this area ranges from Cambrian-Ordovician to Recent. The sequence is composed of alternating clastic and carbonate sequences, and can be differentiated into five major regressive sequences, each of which is terminated by a marine transgression. The overall thickness of the sedimentary sequence gradually increases from about 2 km in the south to as thick as 8 km at the North along the Mediterranean shore [20]. The subsurface stratigraphy of the Palaeozoic section consists of Cambrian-Ordovician, Silurian, Devonian, Carboniferous, and Permian rocks. The lithology of the Cambrian-Ordovician period contains light-colored sandstone with reddish-orange, brick-red, and grey shales, and siltstones. The Silurian sequences are identified using log correlation, which becoming thicker as they move westward. Devonian layers are mostly fine to coarse-grained sandstone, whereas the Carboniferous sediments are represented by the Desouqy and Dhiffah Formations. Dolomite and dolomitic limestone with shale and sandstone interbeds make up the Permian rocks. The Jurassic deposits of the Western Desert have been extensively developed toward the north. The isopach pattern of Middle-Upper Jurassic deposits indicates a prominent east-west tectonic trend, which primarily influenced the accumulation of sediments from the Late Paleozoic period through to the Late Jurassic. [20]. The Western Desert Jurassic Unites are made up of continental as well as marine facies, including Wadi El Natrun, Khatatba, and Masajid formations. Overall, the northern part of the Western Desert stratigraphic succession is an intricate geological record that can provide valuable insights into geological history of the region.

From the given 48 well data (Figure 1.a), the sedimentary sequence in the study area can be separated based on density contrast to their lithologic characters. The five sequences can be identified as follow:

−Sequence I, which is considered the oldest sedimentary rocks, belonging to Palaeozoic and Lower –Middle Jurassic, are dominated by clastic sediments.

−Sequence II, which is belonging to Middle and Upper Jurassic, is a part of carbonate succession.

−Sequence III, which is belonging to the Lower Cretaceous, is made up of another clastic sediments.

−Sequence IV, which is belonging to the Cenomanian at the top of the Middle Eocene, is another carbonate succession.

−Sequence V comprises the Upper Eocene, Oligocene, Miocene, and younger formations. It is a part of the uppermost clastics.

As shown in figure 1b the Miocene sediments cover the majority of the central part of the study area. Limited Pliocene shales and sandstones are exposed in the North. The Pliocene sediments overlie unconformably the Miocene deposits. Eocene rocks cover most of the study area in the South. Meanwhile, in the vicinities of the cultivated fields, Pleistocene and Recent sediments crop out along the Nile Valley. [10]

The primary structural characteristics of the Western Desert, (Figure 2), exhibit orientations spanning from the northeast (NE) to east-northeast (ENE), east-west (EW), and west-northwest (WNW) to northwest (NW). These orientations are a reflection of the dominant geological trends in the basement rock, which encompass two significant patterns oriented along the WNW-ESE and ENE-WSW axes. These geological trends give rise to ENE-WSW depressions and ridges, as described by Meshref [14].

Several prominent elevations in the Western Desert have persisted since the Early Mesozoic Era, such as the Umbarka High, Qattara and Sharib-Sheiba Ridge, Sitra Platform, Bahariya High, and the adjacent Misawag Graben, Ghazalat, and Abu Gharadiq Basins. Conversely, the geological features known as the Meleiha Swell, Dabaa and Mamura Highs, Marmarica Platform, Natrun, and Kattanyia Ridges, along with others, can be attributed to inversion events that occurred during the Senonian-Eocene period, and in some cases, even earlier during the Paleozoic and Jurassic epochs. These events have been well-documented by Sestini, Meshref, and Bayoumi & Lotfy [21] [22] [23], providing evidence of their formation and geological significance.

As described by Guiraud [24], within this region, numerous minor rift basins are present, some dating back to the Permian period, while the majority formed during the Late Jurassic and Early Cretaceous epochs.

The predominant structural configuration within the Western Desert comprises two distinct systems: an underlying series of horst and graben belts characterized by low relief and demarcated by significant master faults with substantial throw, alongside shallower fold structures that originated during the Late Tertiary period, as documented by Sestini [21].

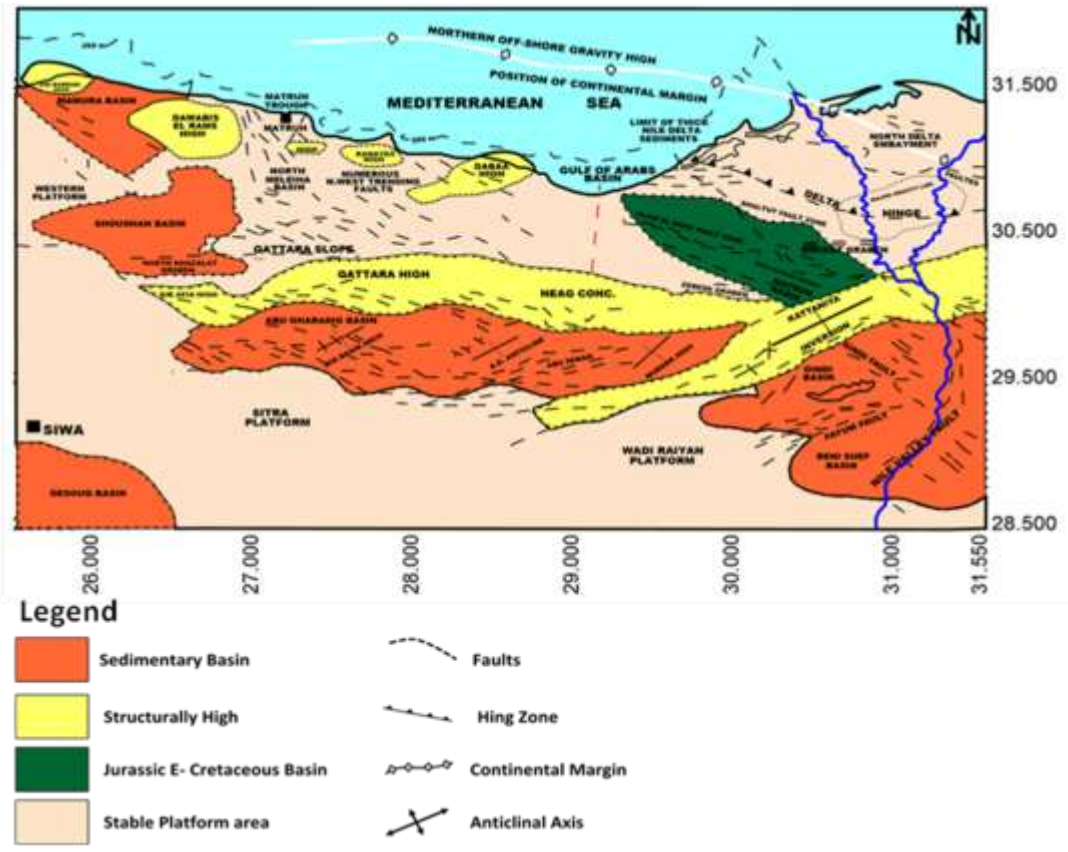

Figure 2: General structure in the Northern Western desert, Egypt, altered after (Bayoumi (23)).

3. Material and Methodology

3.1. Data availability:

The present study was fulfilled using the available geologic and geophysical data as following:

• The Bouguer gravity anomaly map of scale 1:500,000 serve as the format for the geophysical data used in this research. after E.G.P.C. [25]

• Data published in articles including petrophysical parameters and measurements (e.g., [26], [27] and [28]).

• The subsurface data derived from a total of 48 deep wells (as illustrated in Figure 1a), obtained from reputable oil companies, namely: the Egyptian General Petroleum Company (EGPC), the Gulf of Suez Petroleum Company (GUPCO), and the British Petroleum Company (BPC) in the year 2021.

3.2. Gravity data interpretation and processing

Each gravity measurement represents the sum of all effects of combined subsurface features and structures. A gravity map is always a composite of very sharp anomalies, anomalies with intermediate dimensions, and very broad anomalies of a "regional" kind, rather than a single isolated disturbance. As a result, gravity interpretation often starts with a method that isolates the anomalies of interest [29].

The challenging issue in gravity interpretation is separating anomalies of relevance from the overlapping impacts of other features, with deeper features typically causing the most obscuring effects. The difficulty of interpretation is determining the mass distribution responsible for the anomalies, after the concealing interference effects of other characteristics have been eliminated to the best of our ability. [30]

Various techniques can be utilized to remove gravity effects related to unwanted subsurface disturbances. Gravity interpretation by stripping is one of such techniques which filters residual features from regional anomalies. After the effect of the underlying units has been removed, stripping on the tops of lithostratigraphic units implies calculating the gravity effects on these tops, with their sub topographic reliefs. As a result, the structural implications inferred by stripping on are referred to the same timeline, whilst the features deduced by downward continuation convert a particular level into the earth's crust, irrigating the lateral changes of time established through it. [1]

The elimination of the influence exerted by a well-defined density contrast, as determined by independent geophysical and geological data, allows for the computation of gravity values pertaining to other target objects or features of interest. [1]

The gravity stripping process comprises a series of sequential steps. Firstly, the provided data such as the observed Bouguer gravity anomaly map, the geometry of the upper and lower surfaces of any sedimentary sequence obtained from lithologic well logging, and the density of this sequence obtained from the available petrophysical parameters. Secondly, the gravity values of this sequence are calculated, considering the geometrical boundaries and density distribution. Thirdly, the calculated gravity values are eliminated to construct a "stripped" gravity map, which represents the effects from deeper geological structures exclusively. Finally, the regional trend is chosen and removed to produce a residual stripped gravity map for each sequence.

The gravity stripping method involves calculating the gravity effect of a specific depositional sequence, as defined by its varying thickness and density as determined from lithologic log data (Table 1), then subtracting this effect from the integrated effect of the entire sedimentary cover and the underlining basement rocks, as indicated by the Bouguer anomaly map (Figure 2) [31] [32], and so on for the other sequences. The typical equation for stripping various rock units in a sedimentary succession is as follows:

$\Delta g=2\pi G\Delta\rho h$

Where: Δg is the gravity effect of a certain unit in (gal), G is the international gravitational constant, which equals (6.67×10-8 cm3/g. s2), $\Delta\rho$ is the density contrast between the unit density and the basement density (2.67 g/cm3) and h is the thickness of the sequence in cm.

The advantage of the gravity stripping technique is well known for its superior accuracy when compared to mathematical methods, such as convolution for separating the gravitational field (including filtering techniques), as the latter also contains information about the amplification of gravity components that are already there as well as false anomalies. Furthermore, compared to unfiltered gravity signals, all modified (filtered) gravity signals have lower amplitudes. [33] [34]

Seven Bouguer gravity anomaly maps were generated through the application of the stripping technique, with each map corresponding to one of the five designated sedimentary sequences (I, II, III, IV, V), encompassing both the entire sedimentary cover and the basement rocks surface. These maps were constructed after the calculation of the gravity contributions from each individual sedimentary sequence, as illustrated in Figures 3 and 4.

Table 1: The drilled wells in the study area and the thickness of each depositional cycle

Well name	Thickness OF cycle I/ Palaeozoic to Lower Jurassic	Thickness OF cycle 2/ M -U Jurassic	Thickness OF cycle 3/ Lower Cretaceous To Cenomian	Thickness OF cycle 4/'m. Eocene	Thickness OF cycle 5/Recent
Gib Afia-1	528	846	1176	391	130
Bahrein	141 2		1215	412	
N. Ghazalat	533	526	1066	1095	680
Ghourab-1			590	623	684
El Kifar-1	338	73	1705	667	44928
Zarif-1x		31S	1041	209	798
Ras Qattara-1x	51 5	527	880	276	379
Ghazalat-1	728	287	1354	414	229
El Kheit-1		336	1703	595	576
Betty-1	820	12±7	844	675	379
White R.V.H-1			280	660	
Marzuk-1		882	922	454	653
Wü S-1			1074	2174	1147
Aghar-1x			8.76	354	1051
Sonomein-1x			1026	657	1271
Sonhur-1x			979	482	1192
Rabat-1	857			792	546
WD 32-1			400	1977	864
Abu Sennan-1			1436	1073	640
Agnes-I	176	525	797	730	360
Miswag-1	52	1 29	703	90.4	333
Tiba-1x	214	668	544	96	644
WD 12-1		285	886	1782	616
Mubarak-I			1578	994	210
WD 33-1			419	2489	821
S.W. Mubarak-1		403	1378	391	404
WD 57-1	385	452	666	988	482
Diyur-1	464		490	1.76	495
Garif-1		633	700	442	1033
Qattara Rim-1x 1	748	751	467	283	997

Sharib-lx		289	170	473	887
Ghoroud-1x			847	626	973
WD 7-1				2311	1090
WD 7-2				979	930
WD 8-1			1444	1329	933
Abu Ghar-1				1836	1079
Abu Ghar-3				2132	45017
Khatatba-l	22.1	1505.9			366.6
Abu Roash-l	3342	801.4	5939		6.7
Camel Pass W.W.1,2				419.7	448
Wadi Natrun-1	232.7	1145 3	1023.8	667	975.6
El NashFa	183.9		429.4	115.1	
Abyad W. W.,2			2581	86.6	
Agila					309
Gebel Agila				32	97
Wadi El Raiyan No. 1			425.7	831.7	
Abu Ghar-2	793	1866	1018		
BhariyaA-l X	26.8		5095	1885	
Karama 3					

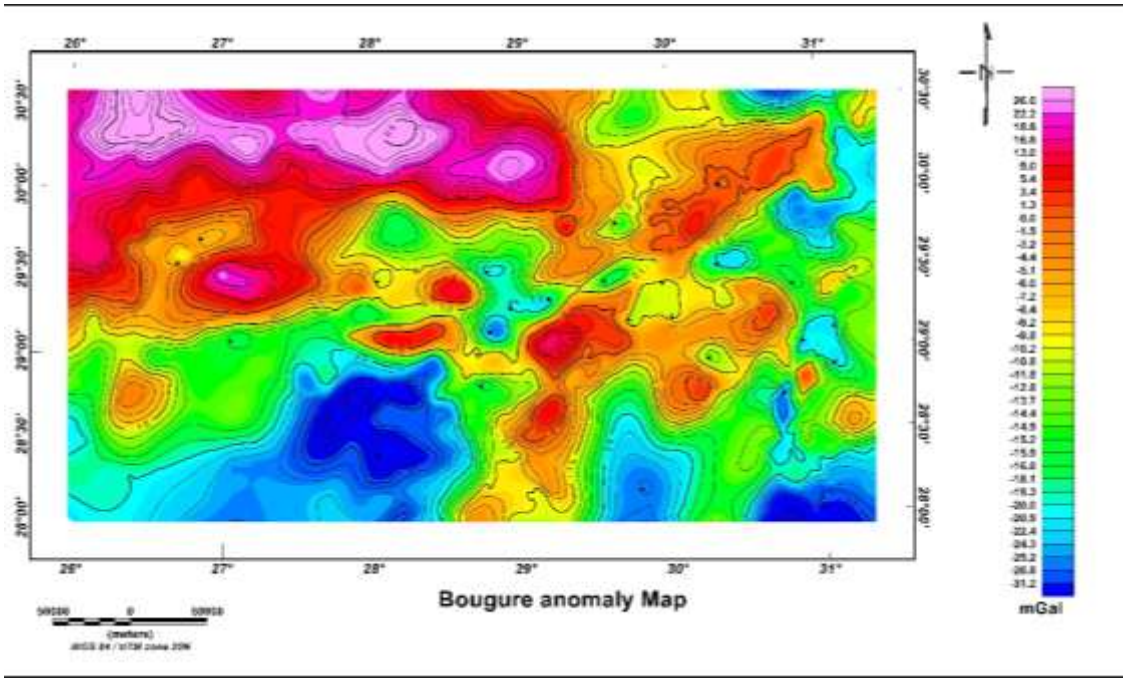

Figure 3: Bouguer anomaly map of the area under study, Western Desert, Egypt (after, E.G.P.C 1987)

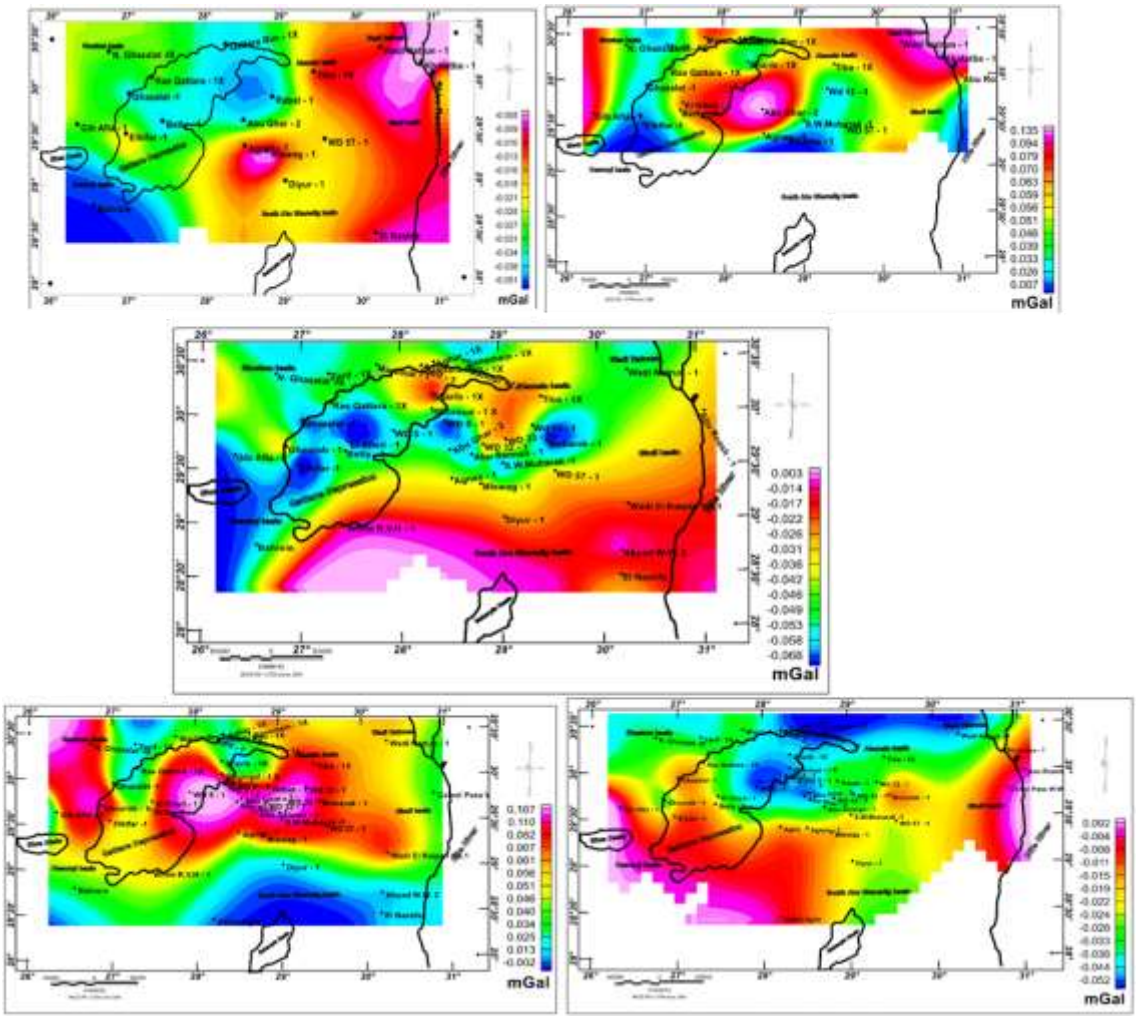

Figure 4: Gravity effect map of different depositional sequences a) sequence I, b) sequence II, c) sequence III, d) sequence IV and e) sequence V.

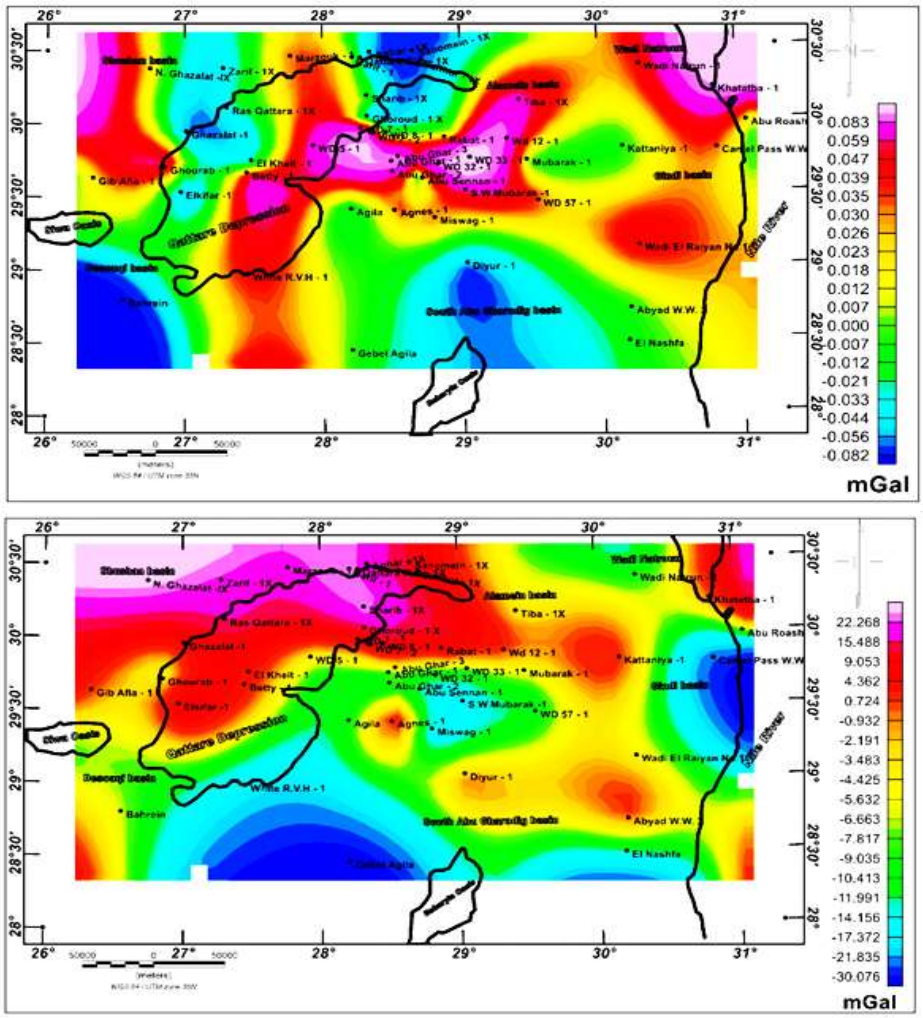

Figure 5: Gravity effect map of a) the entire sedimentary cover b) surface of the basement.

4. RESULTS AND DISCUSSIONS

The qualitative interpretation of Gravity Bouguer anomaly map (figure 3) demonstrates the existence of numerous close anomalies with a wide range of amplitudes, trends, and shapes (such as oval and elongated). The majority of gravity anomalies range in magnitude from -45 to +30 mgal with a notable rising to the northward. Readings of positive gravity anomalies in the north range from 3 to 30 mgal, significantly rising as one proceeds farther north. The negative gravity readings observed in the southern portion have magnitude ranges from -5 to -45 mgal. This indicates two major tectonic units. The northern one began in the Cambrian and continued into the Quaternary and may be indicated by down-faulted blocks of older sediments, [35]. These sediments are saturated with oil and/or gas in places and saline water in other places. A positive gravity anomaly results from the fact that in comparison to the adjacent rocks, these sediments are denser. [36]. Suggesting that the field of gravity increase could be the result of a reduction in crustal thickness to the north. In contrast, most of the sediments in the

southern section are clastic and range in age from the Palaeozoic to the Recent. Most of the significant closed negative anomalies in the southernmost regions are located in the Abu Ghradig and El Ginidi Basins. These are all regarded as an oval -shaped basins. At Abu Ghradig, the local basins inside the main area are represented by these anomalies. The NE-SW and E-W trends are the main linear anomalies in all regions.

Using the stripping technique, we generated seven gravity anomaly maps corresponding to sedimentary sequences labelled as I to V, encompassing the entire sedimentary cover as well as the uppermost layers of basement rocks (Figures 4 and 5). These maps provide a visual representation of gravity values associated with each sedimentary sequence. Sedimentary sequence I, which encompasses the oldest sedimentary rocks spanning the Paleozoic and Lower to Middle Jurassic periods, is featured in Figure 4a. This map illustrates gravity values ranging from -0.07 to -0.007 milli gals (mgal), with distinct low and high gravity values observed in the western and eastern sections of the study area, respectively. The east-to-west gravity variation indicates lateral changes in sedimentary sequence thickness, with a predominant structural trend oriented in the NW-SE direction (as depicted in Figure 6).

Figure 4b displays the gravity anomaly map for sedimentary sequence II, comprising Middle and Upper Jurassic formations. The calculated gravity values in this sequence range from -0.008 to 0.1 (mgal). Notably, sequence II exhibits higher gravity values compared to sequence I due to its composition of denser carbonate rocks, contrasting with the clastic rocks in sequence I. The gravity lineaments inferred from this map (Figure 7) reveal a predominant structural trend oriented in the NW-SE direction.

Figure 4c illustrates the gravity anomaly map for sedimentary sequence III, encompassing deposits from the Lower Cretaceous to the Upper Cretaceous Early Cenomanian, which are significant petroleum reservoirs in the Western Desert. Gravity measurements in this sequence range from -0.07 to -0.002 (mgal). Within the core regions of the study area, circular low anomalies (-0.07 (mgal)) are evident, extending along a north-south axis within the Abu Gharadig basin. Gravity levels increase toward the south. Predominant subsurface structural trends, as inferred from this map (Figure 8), show a NW-SE orientation, with an additional major trend appearing as NE-SW. Low gravity readings suggest an increase in sediment thickness (up to 1400 meters) in these regions, as depicted in Figure 9.

Figure 4d illustrates the gravity anomaly of the sedimentary sequence IV, encompassing deposits from the Cenomanian to the uppermost Middle Eocene. Gravity measurements within this sequence range from -0.002 to 0.167 (mgal). Lower gravity values are observed in the southernmost region of the study area, while the Abu El Gharadig basin exhibits elevated gravity values. The predominant structural trend deduced from this map (Figure 10) extends in a NW-SE direction.

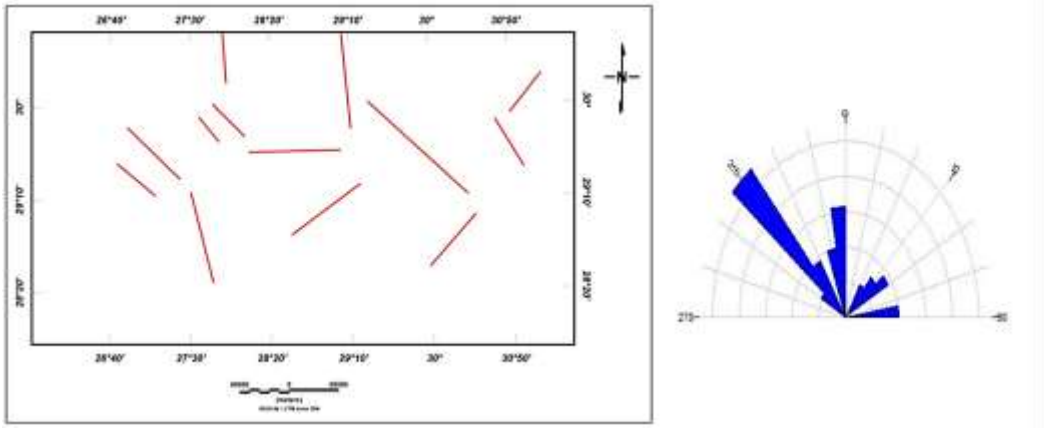

Figure 6: The patterns in gravity lineaments for depositional sequence I as inferred from the stripped gravity map and rose diagram.

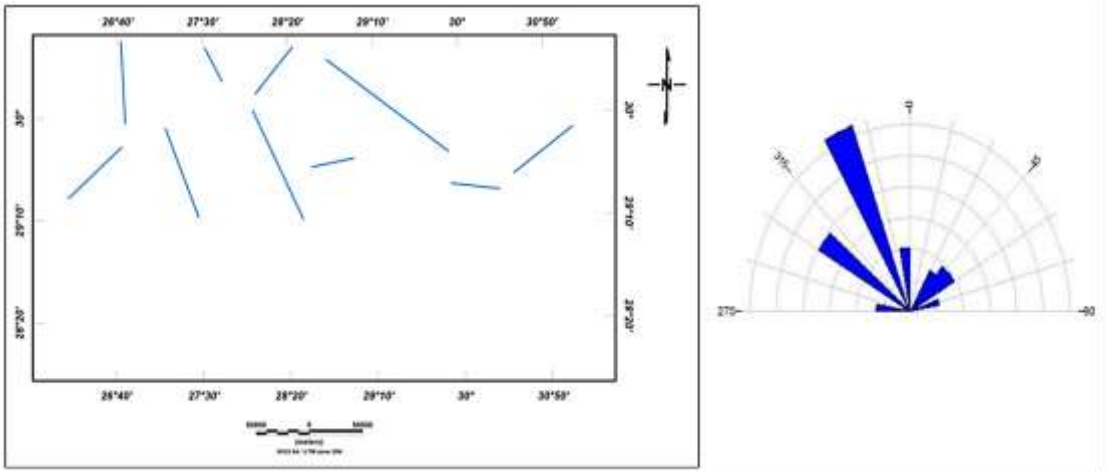

Figure 7: The patterns in gravity lineaments for depositional sequence II as inferred from the stripped gravity map and rose diagram.

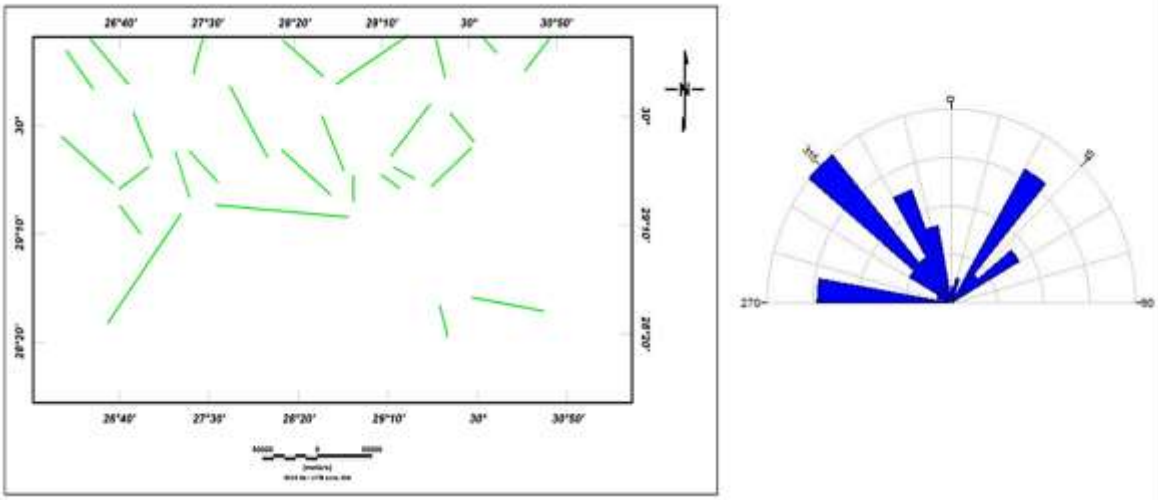

Figure 8: The patterns in gravity lineaments for depositional sequence III as inferred from the stripped gravity map and rose diagram.

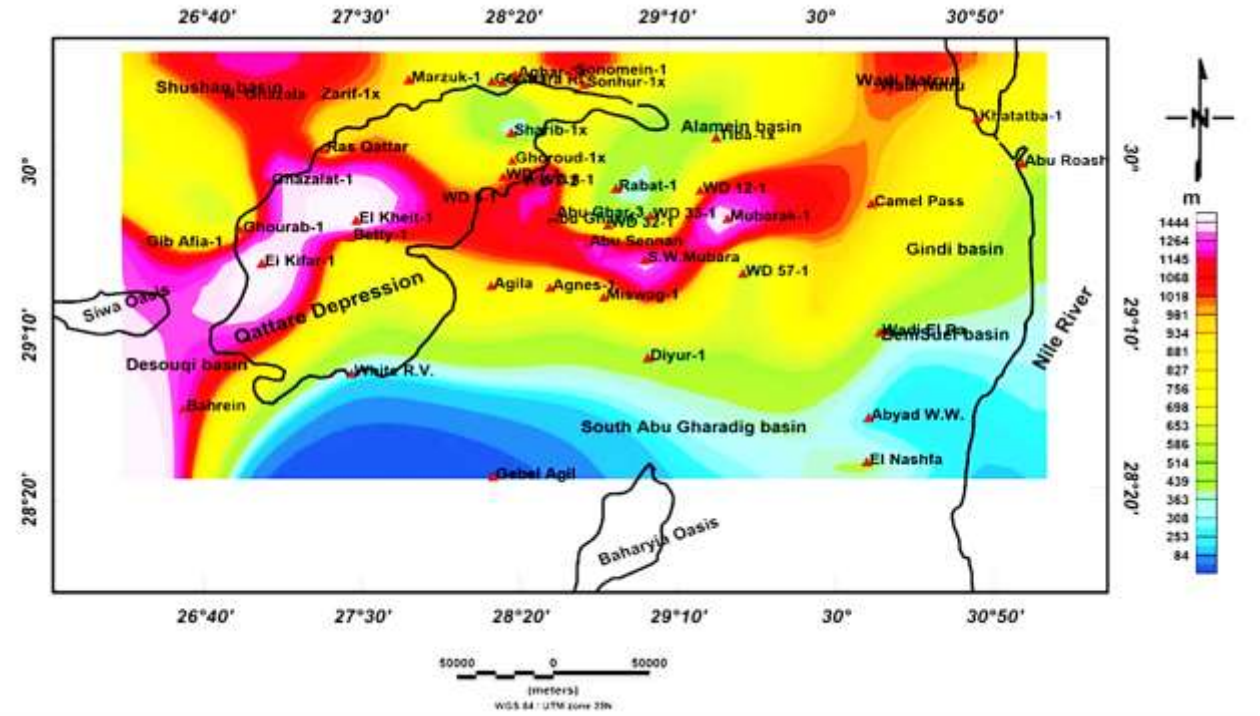

Figure 9: The Isopach map of depositional sequence III.

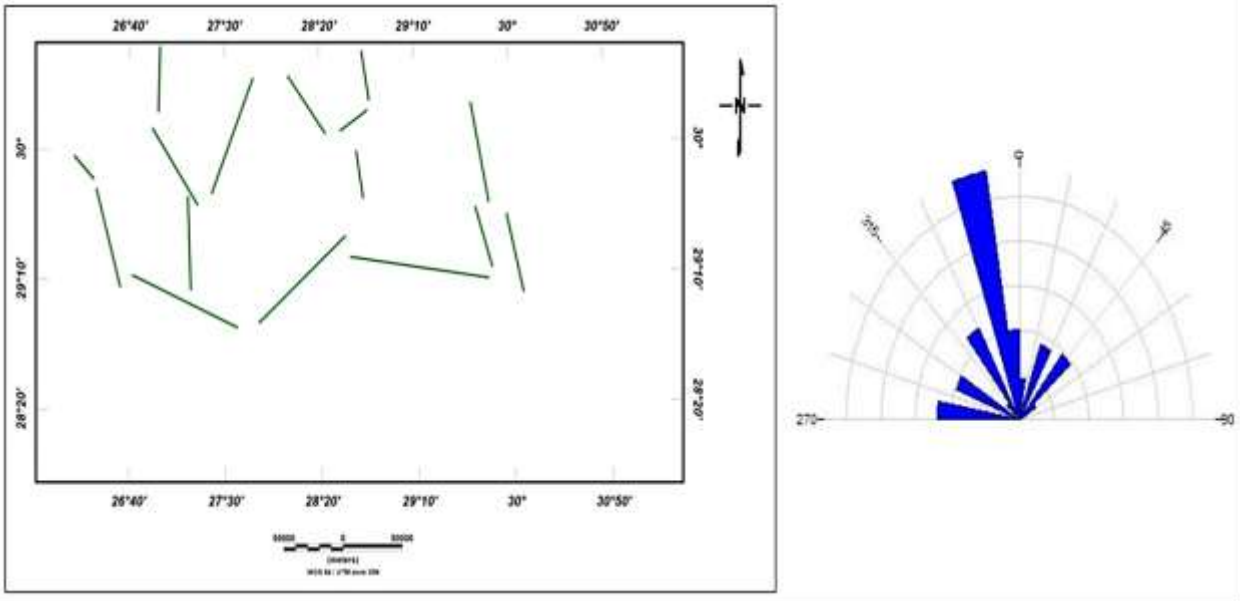

Figure 10: The patterns in gravity lineaments for depositional sequence Iv as inferred from the stripped gravity map and rose diagram.

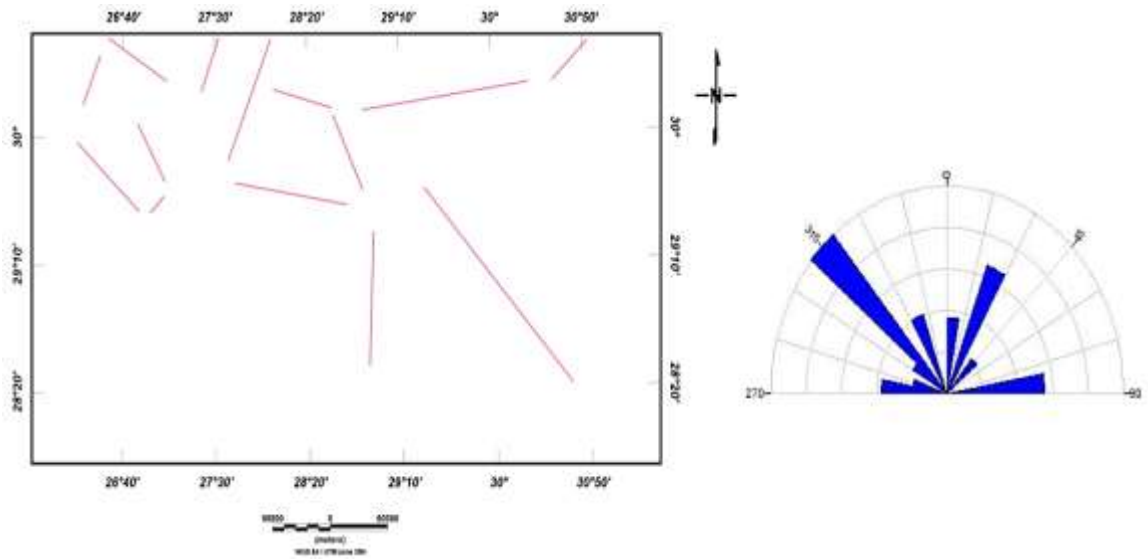

Figure 11: patterns in gravity lineaments for depositional sequence v as inferred from the stripped gravity map and rose diagram.

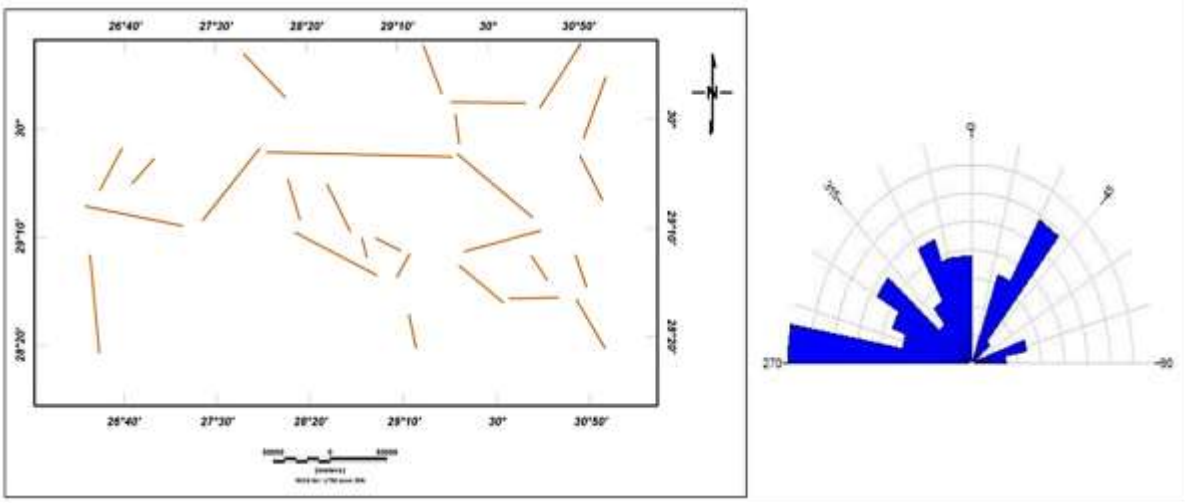

Figure 12: The patterns in gravity lineaments for surface of the basement as inferred from the stripped gravity map and rose diagram.

The clastic sequence V, which includes the Upper Eocene, Oligocene, Miocene, and Recent formations, occur where gravitational values decrease as shown (figure 4e). Gravity readings range from -0.064 to -0.002 (mgal). In the northernmost section of the research area, low gravity values are observed. High computed gravity values are present within the study area at the southernmost extremes. In sedimentary sequence V, the dominant subsurface structural trend is N-W as shown in figure (11). In the meantime, a map of the gravity anomalies throughout the entire sedimentary cover was created by adding the gravity data from all the sedimentary sequences figure (5a). Gravity measurements are between -0.082 to 0.082 mgal. On the other hand, figure (5b) shows the gravitational impact at the top of the basement surface without interference from the sedimentary overlay. The anomalies on this map range in magnitude from -28 mgal in the southern areas to 21 mgal in the research area's northwest. Figure (12) illustrates study

area's gravity fault trend as traced at the top of the basement surface. The dominant structural trends beneath the basement surface are complicated and have different directions than those in the sedimentary cover.

5. CONCLUSION

1. The NW-SE trend is the major subsurface structural predominant trend of the different sedimentary sequences, with a deviation of about 5 degrees eastward or westward from sequence I to Sequence V.
2. The structural trends observed in the basement rocks extend in different directions with some complication compared to those observed in the sedimentary sequences. This indicates that the basement rocks were influenced by an early tectonic phase, and then after the sedimentary sequence had settled another tectonic phase take place and complicated the structures predominating in the basement rocks.
3. The structures in the study area had affected by two tectonic phases. The age dating of these phases cannot be recognized from geophysical data alone but requires more surface and subsurface stratigraphic information.
4. The complicated structures through the previously mentioned two tectonic phases in the study area enhanced the hydrocarbon generation potential, maturation, and accumulation and accordingly production.

6. REFERENCES

[1] **S. Hammer,** Deep gravity interpretation by stripping. Geophysics, 28(3), **(1963)**, 369–378. https://doi.org/10.1190/1.1439186

[2] **A. K. Mohamed, H. H. Ghazala, and L. Mohamed,** Integration between well logging and seismic reflection techniques for structural analysis and reservoir characterizations, Abu El Gharadig basin, Egypt. NRIAG Journal of Astronomy and Geophysics, 5(2), **(2016)**. 362–379. https://doi.org/10.1016/j.nrjag.2016.07.003

[3] **J. P. Beckman,** Mesozoic and Paleozoic stratigraphy of the Western Desert, Egypt, intern. Report, G.P.C., (**1967)**, (R.R., 595).

[4] **P. Norton,** Rock-stratigraphic nomenclature of the Western Desert, Egypt. Int. Report of GPC, Cairo, Egypt, **(1967)**, 557p.

[5] **S. M. Soliman and O. El Badry,** Nature of Cretaceous sedimentation in the Western Desert, Egypt. Review American Association of Petroleum Geologists Bulletin, 34(12), **(1970)**, 2349–2370. https://doi.org/10.1306/5D25CC99-16C1-11D7-8645000102C1865D

[6] **A. S. Abdine and S. Deibis,** Lower Cretaceous Aptian sediments and their oil prospects in the northern Western Desert, Egypt. Eighth Arab Petroleum Congress, Algiers, vol. 74 (B-3), **(1972)**, P.17.

[7] **A. A. Hamed,** Environmental interpretations of the Aptian Carbonates of the Western Egyptian Desert. Eighth Arab Petroleum Congress, Algiers, 79, **(1972)**, (B-3).

[8] **R. Salem,** Evolution of Eocene-Miocene sedimentation patterns in parts of Northern Egypt Review, American Association of Petroleum Geologists Bulletin, 60(1), **(1976)**, 34–64.

[9] **E. M. El Shazly,** The Geology of the Egyptian Region. The Ocean Basins and Margins, springer, vol. 4A, **(1977)**, 379–444. https://doi.org/10.1007/978-1-4684-3036-3_10

[10] **A.A. El-Hussaini, and H. A. Ibrahim,** Gravity interpretation of some sedimentary basins in the Western Desert of Egypt, Bull. Fac. Sci., Assiut Univ., 11(2), **(1982)**, 39-48.

[11] **M. Abu El Naga,** Paleozoic and Mesozoic depocenters and hydrocarbon generating areas, north-western Desert. Proceedings of the 7th Egyptian General Petroleum Corporation, Exploration and Production Conference, Cairo, **(1984)**, 269–287.

[12] **N. Sultan and A. Halim,** Tectonic Framework of northern Western Desert, Egypt, and its effect on hydrocarbon accumulations. EGPC Ninth Exploration Conference, Cairo, Egypt, 2, **(1988)**, 1-19.

[13] **M. L Keeley,** The Paleozoic history of the Western Desert of Egypt, Basin Research, 2, **(1989)**, 35–48.

[14] **W. M. Meshref,** Tectonic framework. In R. Said (editor): The geology of Egypt. Rotterdam, Netherlands, A. A Balkema Publishers, textbook, **(1990)**, 113–155.

[15] **G. Hanter,** North Western Desert. In R. Said, ed., The Geology of Egypt. Rotterdam, Netherlands, A. A. Balkema Publishers, textbook, **(1990)**, 293–319.

[16] **M. A. Hegazy,** Western Desert oil and gas fields (a comprehensive overview). EGPC 11th Petroleum Exploration and Production Conference, Cairo, **(1992)**..

[17] **A. F. Douban,** Basin analysis and hydrocarbon potentiality of Matruh basin, North Western Desert. Egypt. 3rd International Conference of Geology of the Arab World. Faculty of Science, Cairo University, Cairo, Egypt, **(1996)**. 595–624.

[18] **B. Issawi, M. El-Hennawy, M. Francis and A. Mazhar,** Geological interpretation of the main geomorphic units in Egypt. Phanerozoic Geology of Egypt. Geodynamic Approach, The Egyptian Geological Survey, Special Publication No. 76, **(1999)**, 462.

[19] **M. I. Farag,** Geophysical reservoir evaluation of Obaiyed field, Western Desert, Egyp**t,** PhD Dissertation. Technical University of Berlin, Germany, **(2010)**.

[20] **M.L. Keeley and R. J. Wallis,** The Jurassic system in northern Egypt: II. Depositional and tectonic regimes. Journal of Petroleum Geology, 14, **(1991)**. 49–64.

[21] **G. Sestini,** Tectonic and sedimentary history of the NE Africa margin (Egypt - Libya) In Dixon, E.J., Robertson, F. H. A. (Ed.), The geological evolution of the Eastern Mediterranean. Blackwell Scientific Publications, Oxford., 17, **(1984)**, 161–175. https://doi.org/10.1144/gsl.sp.1984.017.01.10

[22] **W. M. Meshref,** Cretaceous tectonics and its impaction on oil exploration in regional Northern Egypt. 'Review Geol. Soc. Egypt, 2(Spec. Publ.), **(1996)**. 199–241.

[23] **A. I. Bayoumi and H. I. Lotfy,** Modes of structural evolution of Abu Gharadig Basin, Western desert of Egypt as deduced from seismic data. Journal of African Earth Sciences, 9(2), **(1989)**, 273–287. https://doi.org/10.1016/0899-5362(89)90070-5

[24] **R. Guiraud,** Mesozoic rifting and basin inversion along the northern African Tethyan margin: an overview. In Macgregor, S.D., Moody, J. T. R., Clark Lowes, D. D. (Ed.), Petroleum geology of North Africa. Geological Society, London., Special Pu **(1998)**., 217–229.

[25] Conoco Coral Geological map of Egypt, scale 1:500,000. The Egyptian General Petroleum Corporation (EGPC), Cairo (1987).

[26] **A. Abdelmaksoud,** Integrated Geological Modelling of The Upper Bahariya Reservoir in Abu Gharadig Oil and Gas Field, North Western Desert, Egypt, Unpublished M. Sc. Thesis, Faculty of Science, Assiut University, Egypt, **(2017)**, 123.

[27] **M. F. Abuhashish, H. A. Wanas and E Madian,** 3D geological modelling of the Upper Cretaceous reservoirs in GPT oil field, Abu Sennan area, Western Desert, Egypt. Journal of Petroleum Exploration and Production Technology, 10(2), **(2020)**, 371–393.

[28] **A. H. Saleh, A. E. Farag, and E. A. Eysa,** Reservoir quality of Abu Roash (G) member in Karama Oil Field, East Bahariya Concession, North Western Desert, Egypt. Arabian Journal of Geosciences, 14(3) **(2021)**, 169. https://doi.org/10.1007/s12517-020-06349-9

[29] **L. L. Nettleton,** Elementary gravity and magnetic for geologists and seismologists: SEG Monograph, Series No. 1, **(1971)**, 121 pp. https://doi.org/10.1190/1.9781560802433

[30] **W. M. Telford, L. P. Geldart, and R. E. Sheriff,** Applied Geophysics (2nd ed.). Cambridge University Press, Textbook, **(1990)**, 770 pp. https://doi.org/10.1017/CBO9781139167932

[31] **I. P. Nedelkon and P. H. Burney,** Determination of gravitational field in depth, Geophysical Prospecting**,** 10, **(1962)**, 1–18. https://doi.org/10.1111/j.1365-2478.1962.tb01995.x

[32] **D. C. Skeels,** An approximation solution of the problem of maximum depth in gravity interpretation, Geophysics, 28(٥), **(1965)**, 724 – 735.

https://doi.org/10.1190/1.1439262

[33] **H. S. Mohamed, M. M. Senosy, and M. Abdel Zaher,** Interactive interpretation of airborne gravity, magnetic, and drill-hole data within the crustal framework of the northern Western Desert, Egypt. Journal of Applied Geophysics, 134, **(2016)**, 291–302.
https://doi.org/10.1016/j.jappgeo.2016.09.002

[34] **H. S. Mohamed, M. M. Senosy, and M. Talat,** Reservoir characterisations from bouguer gravity data, Northern Western Desert, Egypt. NRIAG Journal of Astronomy and Geophysics, 11(1), **(2022)**. 224–236.
https://doi.org/10.1080/20909977.2022.2067680

[35] **R. Said,** The geology of Egypt. Elsevier Publishing Co., Amsterdam, New York, textbook, **(1962)**, 377p.

[36] **MM. El- Gamili,** Regional geophysical investigation, Northern Western Desert, Egypt. PH.D. thesis, Fac. of. Sci., Assiut Univ., Assiut, Egypt, **(1968)**.

[37] **Schlumberger** (1995): Well evaluation conference, Egypt. Schlumberger technical editing services, Chester, p.356.